

Josephson junction oscillators as probes of electronic nanostructures

A. S. Adourian, Scott Yang, and R. M. Westervelt^{a)}

Department of Physics and Division of Engineering and Applied Sciences, Harvard University, Cambridge, Massachusetts 02138

K. L. Campman and A. C. Gossard

Materials Science Department, University of California at Santa Barbara, Santa Barbara, California 93110

(Received 30 June 1998; accepted for publication 14 August 1998)

We have fabricated high-quality planar Nb/AIO_x/Nb Josephson junctions on-chip adjacent to quantum dots in a near surface two-dimensional electron gas in a GaAs/AlGaAs heterostructure. When used as a voltage-tunable oscillator coupled capacitively to a quantum dot, the Josephson junction can produce a localized time-dependent potential of 200 μ V across the dot at frequencies in excess of 300 GHz. The fabrication process involves five separate patterning and processing steps to define the multilayer integrated device. © 1998 American Institute of Physics. [S0021-8979(98)01822-2]

Recently there has been much theoretical and experimental interest in the effects of a high-frequency potential $V_{ac} \cos(2\pi ft)$ on electron transport through small capacitance mesoscopic structures.¹⁻⁸ Investigations in the regime of $hf \gg k_B T$ are expected to yield a multitude of new quantum phenomena. For example, recent experiments on semiconductor quantum dots in the Coulomb blockade regime in the presence of high-frequency (20–30 GHz) time-dependent potentials have demonstrated photon-assisted tunneling where the discrete photon energy becomes observable.⁶ Other time scales for ac transport in semiconductor quantum dots include: the tunneling rate $1/\tau \approx 10$ MHz–10 GHz; the transit time $h/2\pi\Delta \approx 1$ –40 GHz, where Δ is the single particle level spacing; the charging energy $h/(2\pi e/C) \approx 40$ –400 GHz, where C is the total capacitance of the quantum dot; and the plasmon energy $(h/2\pi)\omega_p \geq 1$ THz. A significant challenge in experimentally probing these high-frequency regimes lies in the difficulty of coupling millimeter wavelength electromagnetic radiation to a submicron diameter semiconductor quantum dot.

In this communication we introduce a new approach which integrates a local high-frequency oscillator directly with the device which is under study. It consists of a superconducting Josephson junction incorporated on-chip with a quantum dot which is formed electrostatically in a near surface two-dimensional electron gas (2DEG). The Josephson junction is a natural high-frequency voltage-tunable oscillator which is fabricated adjacent to the quantum dot. By means of an integrated transmission line coupling structure, the oscillating Josephson voltage signal can be capacitively coupled to the electron gas. The resulting high-frequency potential is strongly confined to the submicron active region of the quantum dot. We have developed a successful fabrication process and have demonstrated high-quality Josephson junction oscillators integrated with semiconductor quantum dot devices.

A scanning electron micrograph of a completed integrated thin-film Josephson junction and quantum dot device is shown in Fig. 1(a), and a schematic of the structure is shown in Fig. 1(b). The device consists of six metallic Cr:Au gates which are used to electrostatically define the quantum dot, one Josephson junction trilayer, and the structure used to couple them at rf frequencies. The substrate is a GaAs/AlGaAs heterostructure containing a high-mobility 2DEG 470 Å beneath the surface. Fabrication of a completed device involves five successive patterning and processing steps aligned to within 100 nm of each other. The patterning is done by electron-beam lithography on a bilayer poly(methylmethacrylate) (PMMA) resist using standard liftoff techniques.

In order to maximize both the oscillation frequency and the output power of the Josephson oscillator, high current density tunnel junctions with large superconducting energy gaps are desirable. The Josephson junction in our device is a Nb/AIO_x/Nb trilayer which was deposited in a dc plasma sputtering system in 10 mT of Ar without breaking vacuum. By sputtering the Al layer at a rate of 60 Å/min, pinhole-free AIO_x tunnel barriers of 30 Å thickness were deposited which resulted in high critical current densities of 1000 A/cm².^{9,10} An AIO_x barrier was chosen because of its excellent stability and low dielectric constant.⁹ The final $10 \times 10 \mu\text{m}^2$ junction is defined by a SF₆ reactive ion etch of the top Nb counter electrode using PMMA as an etch mask. This etchback of the top Nb layer also serves to eliminate any electrical shorting which may have existed across the edges of the junction due to liftoff imperfections. As seen in Fig. 1, an insulating SiO_x layer is then thermally deposited over two edges of the Josephson junction. This prevents shorting of the trilayer by the top Au layer which forms the electrical contact to the Nb counter electrode. The insulating SiO_x layer and the top Au layer also extend across the gates used to define the quantum dot in the 2DEG. Together with the bottom Au layer under the Nb base electrode this extension forms a transmission line which is capacitively coupled to the source and drain electrons in the 2DEG quantum dot. The top and bottom Au

^{a)}Electronic mail: westervelt@deas.harvard.edu

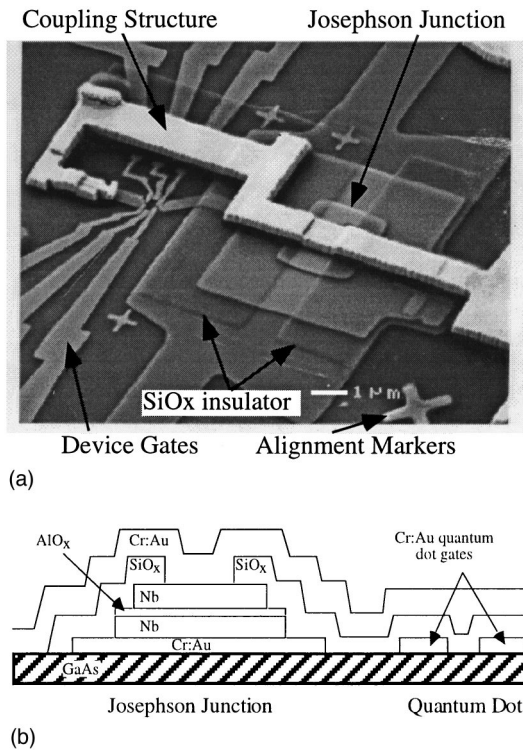


FIG. 1. (a) Scanning electron micrograph of completed multilayer device indicating various features. (b) Schematic of integrated thin-film device. The vertical scale is greatly exaggerated for clarity.

layers also aid in the removal of heat from the junction area to minimize self-suppression of the superconducting energy gap in the Nb electrodes under bias.

A typical current–voltage ($I_{\text{bias}}-V_{\text{dc}}$) curve of an on-chip $10 \times 10 \mu\text{m}^2$ Josephson junction at 4.2 K is shown in Fig. 2. The observed gap sum value ($2\Delta = 2.3 \text{ mV}$), a measure of the quality of the Nb films, is somewhat reduced compared to the clean Nb value of $2\Delta(0) = 3.1 \text{ mV}$ (Ref. 11) due to the proximity effect with metallic Al in the barrier and impurities in the Nb film. The normal state resistance and the critical current of the junction are measured to be $R_n = 1.2 \Omega$, and $I_c = 0.9 \text{ mA}$, respectively. As is expected for a planar geometry, the junction capacitance leads to a hysteretic current–voltage curve symmetric about the origin. When

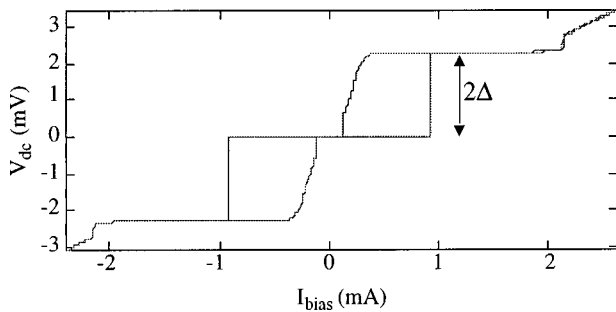


FIG. 2. $I-V$ characteristic of $10 \mu\text{m} \times 10 \mu\text{m}$ Josephson junction at 4.2 K, $I_c = 0.9 \text{ mA}$, $R_n = 1.2 \Omega$.

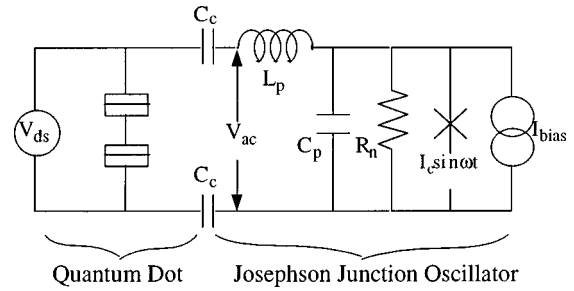


FIG. 3. Equivalent circuit model of Josephson junction/quantum dot device.

a dc voltage bias is applied across the Josephson junction it will produce an oscillating voltage signal at a frequency determined by the Josephson relation

$$f = 2eV_{\text{dc}}/h, \tag{1}$$

where V_{dc} is the average dc voltage across the junction. Experimentally, we current bias the Josephson junction so that $V_{\text{dc}} = I_{\text{bias}}R_n$, where I_{bias} is the applied current bias. An upper limit on the operating frequency of our Josephson oscillator is set by the superconducting gap of the Nb, which in this case corresponds to 1.1 THz; a typical operating frequency is 300 GHz, corresponding to $V_{\text{dc}} \approx 1 \text{ mV}$ in Fig. 2. At this frequency the signal wavelength is $\lambda = 380 \mu\text{m}$, taking into account the dielectric constant of the GaAs half-plane $\epsilon_{\text{GaAs}} = 13.1$ [$\lambda = \sqrt{2/\epsilon_{\text{GaAs}} + 1}$], which is much longer than the $10 \mu\text{m}$ length of the transmission line between the Josephson oscillator and the quantum dot. As a result, the phase of the signal across the length of the coupling structure is approximately constant and we may use a simple ac circuit to model the device.

The equivalent circuit of the integrated Josephson oscillator and quantum dot is shown in Fig. 3. L_p and C_p are the parasitic inductance and capacitance of the combination of the planar Josephson junction and the transmission line coupling structure, and C_c represents the coupling capacitance between the open end of the transmission line structure and the electrons in the 2DEG 470 \AA beneath the surface. For the dimensions shown in Fig. 1, we estimate a parasitic inductance of $L_p = 1.3 \text{ pH}$. The magnitude of the oscillator signal across the dot, V_{ac} , will be determined by the total capacitive loading of the Josephson oscillator. When the McCumber parameter β_c , defined as¹¹

$$\beta_c = (4\pi e/h)(I_c R_n)(R_n C_p), \tag{2}$$

is less than unity the junction is not capacitively shunted and the maximum ac voltage obtainable is $V_{\text{ac}} \approx I_c R_n = 1.1 \text{ mV}$, at least for $V_{\text{dc}} < 2\Delta/e$. The capacitance C_p in Eq. (2) is dominated by the capacitance of the planar junction. For a $10 \times 10 \mu\text{m}^2$ trilayer junction with an AlO_x barrier 30 \AA thick this capacitance is $C_p = 2.1 \text{ pF}$, using $\epsilon_{\text{AlO}_3} = 8$ for the dielectric constant of the AlO_x barrier. This gives $\beta_c = 7$, so

the ac voltage signal is partially shunted with the 3 dB point at 80 GHz, and the $I-V$ curve is hysteretic. Using this value of β_c , at a typical operating frequency of 300 GHz the magnitude of the oscillating potential expected across the quantum dot in the circuit model is approximately $200 \mu V$.

In summary, we have presented a novel device which integrates on-chip a Josephson junction oscillator and a semiconductor quantum dot with coupling structures. We have developed a process for fabricating these multilayer integrated devices which results in high-quality Josephson junctions with characteristics well suited to their use as high-frequency sources. By coupling an on-chip oscillator to a single mesoscopic device we may eliminate the need for external sources of radiation and avoid the difficulties involved with transmitting a high-frequency signal into a millikelvin cryostat. In the future it may be possible to build on-chip Josephson oscillators with frequency ranges extending from a few hundred gigahertz to over 1 THz, allowing the study of a variety of time-dependent phenomena in electron transport through mesoscopic structures.

This work was sponsored at Harvard by Grant Nos. ONR N00014-89-J-1592, JSEP N00014-89-J-1023, and at UCSB by Grant No. AFOSR-91-0214.

- ¹K. Flensberg, S. M. Girvin, M. Jonson, D. R. Penn, and M. D. Stiles, *Phys. Scr.* **T42**, 189 (1992).
- ²K. K. Likharev and I. A. Devyatov, *Physica B* **194–196**, 1341 (1994).
- ³A. Hadicke and W. Krech, *Physica B* **193**, 256 (1994).
- ⁴C. Bruder and H. Schoeller, *Phys. Rev. Lett.* **72**, 1076 (1994).
- ⁵Q. Hu, *Appl. Phys. Lett.* **62**, 837 (1993).
- ⁶L. P. Kouwenhoven, S. Jauhar, K. McCormick, D. Dixon, and P. L. McEuen, *Phys. Rev. B* **50**, 2019 (1994).
- ⁷R. H. Blick, R. J. Haug, J. Weis, D. Pfannkuche, K. V. Klitzing, and K. Eberl, *Phys. Rev. B* **53**, 7899 (1996).
- ⁸P. S. S. Guimaraes, B. J. Keay, J. P. Kaminski, S. J. Allen, P. F. Hopkins, A. C. Gossard, L. T. Florez, and J. P. Harbison, *Phys. Rev. Lett.* **70**, 3792 (1993).
- ⁹M. Gurvitch, M. A. Washington, and H. A. Huggins, *Appl. Phys. Lett.* **42**, 472 (1983).
- ¹⁰S. Morohashi, F. Shinoki, A. Shoji, M. Aoyagi, and H. Hayakawa, *Appl. Phys. Lett.* **46**, 1179 (1985).
- ¹¹T. P. Orlando and K. A. Delin, *Foundations of Applied Superconductivity* (Addison-Wesley, Reading, MA, 1991).